

5-2018

The Mechanisms of Pond Expansion in the Marshes of Blackwater National Wildlife Refuge, Maryland

Joshua Himmelstein

Follow this and additional works at: <https://scholarworks.wm.edu/honorstheses>



Part of the [Biogeochemistry Commons](#), [Geomorphology Commons](#), [Hydrology Commons](#), and the [Terrestrial and Aquatic Ecology Commons](#)

Recommended Citation

Himmelstein, Joshua, "The Mechanisms of Pond Expansion in the Marshes of Blackwater National Wildlife Refuge, Maryland" (2018). *Undergraduate Honors Theses*. Paper 1216.

<https://scholarworks.wm.edu/honorstheses/1216>

This Honors Thesis is brought to you for free and open access by the Theses, Dissertations, & Master Projects at W&M ScholarWorks. It has been accepted for inclusion in Undergraduate Honors Theses by an authorized administrator of W&M ScholarWorks. For more information, please contact scholarworks@wm.edu.

**The Mechanisms of Pond Expansion in the Marshes of the Blackwater National
Wildlife Refuge, Maryland**

A thesis submitted in partial fulfillment of the requirement for the degree of Bachelor of
Science in Geology from
The College of William and Mary

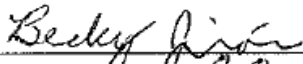
by

Joshua Himmelstein

Accepted for **High Honors**

 Matthew Kirwan, Director

 Greg Hancock

 Becky Jiron

 Randolph Chambers

Williamsburg, VA
May 4, 2018

Table of Contents

Abstract.....	2
Introduction	
1.1 <i>Background</i>	3
Methods	
2.1 <i>Site Description</i>	4
2.2 <i>Historical Methods</i>	7
2.3 <i>GIS Study Sites</i>	7
2.4 <i>GIS Methods</i>	8
2.5 <i>Expansion and Merging calculations</i>	9
2.6 <i>Fieldwork overview</i>	9
2.7 <i>Soil Strength</i>	10
2.8 <i>Biomass</i>	11
2.9 <i>Porewater Chemistry</i>	12
Results	
3.1.1 <i>Changes in Pond Area</i>	13
3.1.2 <i>Pond Size Distributions</i>	15
3.1.3 <i>Expansion vs Merging growth rates</i>	16
3.1.4 <i>Non-merging ponds growth rates</i>	17
3.2 <i>Characteristics of stable and unstable ponds</i>	18
Discussion.....	21
Conclusion.....	24
Acknowledgements.....	25
References Cited.....	26

Abstract:

Many saltmarshes throughout the world are converting to open water through the development and expansion of ponds. High rates of relative sea level rise are leading to widespread marsh submergence and ponding in the 28,000-acre microtidal Blackwater National Wildlife Refuge (Maryland, USA), but knowledge of the mechanisms involved is limited. Here, we use historic aerial imagery and field-based measurements to quantify pond development and identify the processes involved. Historical photograph analyses indicates that many small ponds emerge on the marsh platform and quickly merge with other nearby ponds, slowing their growth rates with size. A consistent rate of marsh loss in each study area suggests biogeochemical mechanisms such as organic matter decomposition drive pond expansion. Biomass, porewater chemistry, and soil strength measurements from marshes adjacent to stable and unstable ponds suggest pond growth rates are related to surrounding marsh health. Finally, this study finds that the merging of small, unstable ponds rather than the continued singular expansion of large ponds is the primary driver of pond expansion in the Blackwater marshes. .

Introduction

1.1 Background

Marshes are important ecosystems that physically and chemically protect the world's coasts. They buffer cities from storm impacts, sequester atmospheric carbon, remove excess nutrients from fertilization runoff, and provide rich habitats for fish and wildlife. In 2008, a leading report valued existing US coastal wetlands at USD 23.2 billion yr^{-1} (Costanza et al., 2008). As of 2010, 39% of American's lived in coastal counties, many of which rely on the socioeconomic value of these wetlands (National Ocean Service, 2013). Climatic and local changes pose major threats to saltmarshes and associated cities, threatening to weaken these vital ecosystems. While marshes depend on cyclical flooding to form and grow, rates of sea level rise (SLR) greater than rates of marsh accretion can effectively drown marshes (Reed, 1995). A second change – reduction of sediment supplies due to upstream trapping or diversion – weakens a marsh's dynamic ability to keep up with SLR. Marshes are adaptive ecosystems that can persist via inland migration and vertical growth, but in some instances their rate of adaptation is insufficient for survival (Kirwan et al., 2010).

Ponding is a prevalent and increasing feature of saltmarshes and is thought to be a primary driver of marsh loss in submerging marshes, converting the vegetated marsh platform to lower elevation pools and mudflats (Kearney et al., 1988; Nyman et al., 1994; Mariotti and Fagherazzi 2013; Wang and Temmerman 2013; Mariotti 2016; Schepers et al. 2016). These two contrasting ecosystem states exist at separate elevations in the tidal frame and are characterized by different feedback mechanisms. Inundated vegetation on the elevated marsh slows water velocities and promotes sediment deposition. Marshes inundated for longer durations experience increased deposition and may be able to keep pace with sea level rise. (Pethick 1981; Allen 1990; French 1993; Vandenbruwaene et al. 2011). Another dynamic feature of the marsh ecosystem state is autochthonous organic sedimentation from the death and decomposition of above and below-ground plant matter.

Ponds can form through a variety of physical and biogeochemical initiators – the process always begins with a local loss of vegetation. Physically, ponds can form through bioturbation or herbivory, creek blockage, ice scouring, and wrack deposits (Pethick, 1974; Wilson et al., 2014). Ponds may also initiate biogeochemically by waterlogging stress, whereby organic senescence and subsequent degradation weakens a once cohesive area of marsh. Biogeochemical processes depend on elevation, hydroperiod, landscape gradient, and the overall hydrologic conductivity of a marsh. This form of die-off is prevalent in marshes with low relief, low tidal range, and increased flooding duration due to sea level rise (Wilson, 2014).

Once formed, ponds can either enlarge or recover to become marsh again. The likelihood of recovery depends on conditions such as sediment exchange, tidal range, and water quality – all related to tidal connection. Connections allow suspended sediments and nutrients to enter a pond system as water level fluctuates, but also permit more frequent sediment export. Ponds larger than a site-dependent critical width are prone to runaway expansion whereby wave-induced edge retreat produces a positive growth feedback; as ponds enlarge wave-power increases along with its potential to erode a pond's margin (Mariotti and

Fagherazzi, 2013). Ponds smaller than this threshold width may grow through a suite of poorly defined biochemical and physical mechanisms such as peat collapse through decomposition, edge creep, or current-induced sediment export. The processes by which expansion occurs vary with pond size and connection and are poorly understood. This study tests the hypotheses that the conjoining, or merging, of two or more ponds is a primary mechanism of marsh loss and that a pond's stability is reflected by the characteristics of its surrounding marsh.

Methods

2.1 Site Description

The Blackwater National Wildlife Refuge (Blackwater NWR) is a 28,000-acre refuge that contains a 1/3rd of Maryland's tidal wetlands and exhibits extensive ponding (Figure 1). Established in 1933 for its importance as a migratory waterfowl stopover and wintering grounds, the Refuge and its marshes support a diverse animal community. Before its eradication, the invasive Nutria was a member of this community whose intensive herbivory is associated with marsh loss in the Blackwater NWR. Their destructive feeding habits in concurrence with sea level rise have resulted in the loss of over 5,000 acres of saltmarsh in the past 40 years of the Refuge's life, and some 50% of all the refuge's marshes since the 1930s.

The drastic and seemingly irreversible pondage along with the high sea level rise (SLR) recorded in the Refuge make it a valuable contemporary study site which provides insights into the future conditions of other wetlands. Historic relative SLR measured at the nearby NOAA Cambridge, Maryland monitoring station is 3.70mm/year +/- 0.32 mm/year (NOAA Station 8571892, <http://tidesandcurrents.noaa.gov/sltrend>, 10/9/2017). This rate is higher than the average accretion rates of 1.7-3.6mm/year measured in the Blackwater NWR (Stevenson et al. 1985). Accretion rates vary across marshes, and the tidal conditions of the Blackwater NWR

vary with distance from Fishing Bay to the Southeast. The spring tide range is over 1.0m in Fishing Bay and attenuates to less than 0.2m at Lake Blackwater ~10km northwest from the

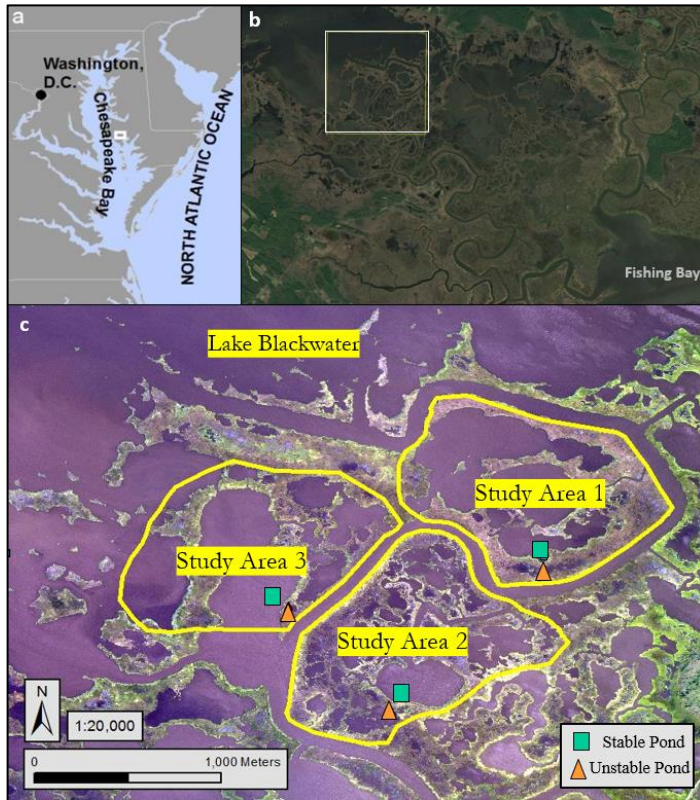


Figure 1 – a.) Location of Blackwater Wildlife Refuge outlined by a white square on Eastern edge of Chesapeake Bay; b.) Overview of the 28,000 acre refuge, evidencing vegetation die-off and marsh loss following gradient from low die-off near southeastern Fishing Bay to high die-off near Lake Blackwater at the northwest reaches of Blackwater River; c.) The three study areas used for remote sensing analyses with the field-sampled ponds indicated within; false-color 2015 infrared Imagery.

ponds expand and lead to permanent marsh loss (Stevenson et al., 1985). Past research conducted on the gradient suggests three processes that could result in the visibly waevident pattern (Schepers et al., 2016). First, a decrease in suspended sediment concentration away from Fishing bay is correlated with reduced sedimentation and reduced vertical marsh growth. Second, wind-driven wave erosion erodes and resuspends sediments in the large Lake Blackwater, and dominant northwesterly winds carry the sediment downstream and into Fishing Bay (Ganju et al. 2013, 2015). As the suspended sediment is carried downstream a portion of it may be deposited on the marsh levees and platforms adjacent to the Blackwater River, aiding in the persistence of these marshes. Third, the shrinking tidal amplitude from 1.0m near Fishing Bay to 0.2m in Lake Blackwater narrows the effective elevation range for tidal vegetation to grow in. Due to lag time and local bathymetry, tidal range decreases with distance from the bay and the capacity of the marsh to compete with SLR decreases (Kirwan

bay. The tidal Blackwater River connects the two and carries sediment and nutrients from the bay towards Lake Blackwater during flood tides. The Little Blackwater River to the west of Lake Blackwater is an upstream input of freshwater and suspended sediment to the Refuge. This tributary is not a large supply of sediment – suspended sediment concentrations (SSC) are normally less than 10mg/L (Ganju et al., 2013), and most sediment is contributed either through resuspension within the refuge or from Fishing Bay (Ganju et al., 2013). The narrow tidal range experienced by the marshes can be exaggerated during storm events, when barometric pressure changes and strong winds can change water levels by over 1.0m (Wang and Elliot, 1978).

The conversion from vegetated marsh to unvegetated ponds and mudflats in the Refuge follows a gradient along the Blackwater River, from extensive die-off around the Lake Blackwater to minor die-off near Fishing Bay (Figure 1). In Blackwater, almost all

and Guntenspergen 2010; Kirwan et al. 2010; D'Alpaos et. al 2011). The compounding effects of low suspended sediment concentrations, net sediment export, and a minimal tidal compensation range yield higher ponding rates nearer to Lake Blackwater.

The Refuge's marshes are characterized by mesohaline vegetation which grows in brackish waters. Low elevation areas of the refuge, like those that surround many ponds, are dominated by the sedge plant *Schoenoplectus americanus* and the cordgrass *Spartina alterniflora*. Intermediary elevation areas found throughout the marsh are composed of *Distichlis spicata* and *Spartina patens*. High elevation areas are characterized by *Spartina cynosuroides* and *Phragmites*.

2.2 Historical Methods

To determine spatiotemporal patterns of pond growth I performed GIS analyses on historic aerial images of the Blackwater NWR. Imagery from 1938, 1981, and 2010 was sourced from a previous project by Schepers et al. (2016). Imagery from the year 1960 was acquired from the USGS Earth Explorer to gain higher temporal resolution during a period when pondage in the refuge increased drastically (Table 1). This imagery was georeferenced by tethering fixed points such as road intersections with the previously georeferenced imagery and performing a spline transformation to optimize the projection. All imagery was then georectified and projected in the NAD 1983 UTM Zone 18N. To minimize the effect of varied image quality, all images were resampled to the coarsest image resolution of 1.55m per pixel edge.

Image Year	Image Type	Resolution (m)	Source	Digitization
1938	Black and white	0.86	Scott et al. (2009)	Manual
1960	Black and white	1.55	USGS Earthexplorer	Digital
1981	Color infrared	1.55	USGS Earthexplorer	Manual
2010	Visible + NIR	0.3	Blackwater NWR	Digital

Table 1 – Overview of imagery used for remote sensing analyses, with pre-resampled resolutions shown.

2.3 GIS study sites

We analyzed 3 study areas adjacent to the northwest reaches of the Blackwater River to track individual ponds through time and test spatial differences between study areas. I selected this region of Blackwater NWR because it experienced some of the most rapid pond growth in all the refuge, and because it was recently studied and classified by Schepers et. al (2016). Study areas, clustered near one another, are ~800,000m² and border the meanders of the Blackwater River. The areas each feature a large, connected central pond in the 1938 imagery which may act as internal source of sediment along with the Blackwater River – although accretion in the Refuge is dominated by root accumulation and organic sedimentation (Rocchio, 2017).

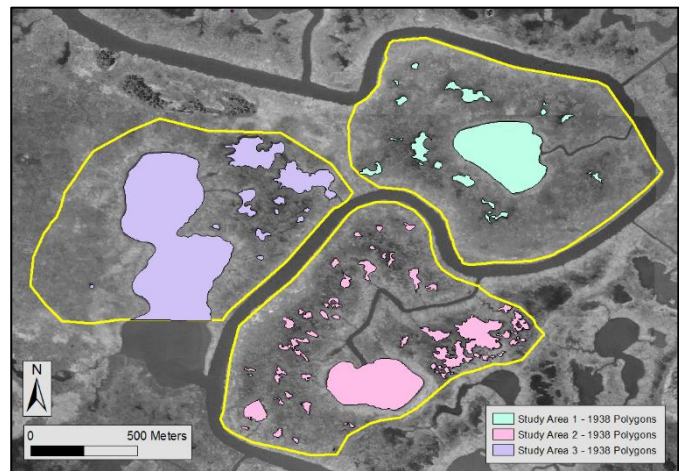


Figure 2 – Three study areas along Blackwater River, outlined in yellow. User-delineated 1938 pond polygons shown in color to illustrate ponds of interest.

2.4 GIS methods

Pond delineation completed by Schepers et. al (2016) manually classified all ponds greater than 50m² in the 1938 (Figure 2) and 1981 images of the Refuge and used a maximum likelihood classification (MLC) to draw ponds for the 2010 imagery. I further completed a MLC for the 1960 image in ArcGIS to differentiate water from marsh. This classification method utilizes user input 'signatures' where known water and known marsh are drawn and assigned opposing values. The program then assigns values to the rest of pixels based on which 'signature' each pixel most resembles. The raster layer output by this method is finally converted into a polygon layer where adjacent pixels of the same classification merge to form polygons representing water. This method was verified by Schepers et. al (2016), who found a 97% accuracy (based on ground verification points) for their 2010 classification. Ground verification was not completed for the 1960 classification, but a visual comparison to the original imagery showed reasonable but jagged classification in all areas except study area 2, where prescribed burning blackened the northwest portion of the marsh there. A manual touch-up of pond polygons in my 3 study areas smoothed and extended polygons to the visible boundary of the water as previous polygons were conservatively classified (Schepers et. al, 2016). I then clipped all pond polygons to be contained within the study areas, and used the statistics function in ArcGIS to calculate the area of each polygon. Pond areas were transcribed into Excel and given an ID number representing their identity and pattern of growth. If a pond appeared to grow by simple edge expansion, it maintained an integer ID (eg. 23). If a pond at a later timestep overlapped two previous ponds I assumed those ponds merged in the formation of the larger pond – and thus the new pond was given an integer ID followed by the number of ponds enveloped in it (eg. 14.2). This identification scheme allowed for individual pond IDs that carried information about past growth patterns. Total ponded counts and total pond area were recorded in each polygon at each timestep for use in expansion and merging calculations.

2.5 Expansion and merging calculations

To calculate study-area-averaged rates of pond growth due to simple edge expansion versus rates of pond growth due to merging, I derived dynamic area/year equations that characterize the two separate end member mechanisms of pond growth. The first limiting case is that of no pond merging despite pond expansion, represented by a fixed number of ponds with a changing area ($n_o = n_f$; $A_o \neq A_f$). The other limiting mechanism is pond merging whereby ponds join, reducing the number of ponds but occupying a fixed area ($n_o \neq n_f$; $A_o = A_f$). Neither extreme exists alone, and together these extremes equal the total rate of ponded area growth. The opposing cases are expressed in the $R_{\text{expansion}}$ and R_{merging} equations; these rates are additive and can be used to extract the merging and expansion contributions of arbitrary changes in area (A) and pond number (n). This model functions properly when the total ponded area grows between timesteps and when the number of ponds decreases or remains the same. Due the latter constraint, only ponds overlapping those existing in 1938 were included for this portion of the analysis. Variables below are defined as follows:

- A_o = Initial ponded area in study area (m^2)
- A_f = Final ponded area in study area (m^2)
- n_o = Initial number of ponds over 50 m^2 in study area (unitless)
- n_f = Final number of ponds over m^2 in study area (unitless)
- Δt = change in time between imagery dates (years)
- R_x = rate of change (m^2 / year)

$$1.) \text{ Rate of total pond area growth} = R_{\text{pondareagrowth}} = \frac{\frac{A_f}{n_f} - \frac{A_o}{n_o}}{\Delta t}$$

assuming $A_o \leq A_f$ and $n_o \geq n_f$

$$a.) \text{ Rate of ponded area growth due to expansion} = R_{\text{expansion}} = \frac{\frac{A_f - A_o}{n_o}}{\Delta t}$$

$$b.) \text{ Rate of ponded area growth due to merging} = R_{\text{merging}} = \frac{\Delta n}{n_o \Delta t} * \frac{A_f}{n_f}$$

$$c.) R_{\text{expansion}} + R_{\text{merging}} = R_{\text{pondareagrowth}}$$

2.6 Fieldwork overview

To assess pond growth and stability in ways that cannot be addressed through remote sensing, I performed fieldwork in the Blackwater NWR sampling and collecting geomorphic and biological indicators of marsh health including soil strength, above-ground biomass, porewater chemistry, and soil organic content and bulk density. In each study area I selected two adjacent ponds to sample – one stable and one unstable as defined by annual areal growth rates of less than 1% and greater than 1% respectively. Ponds were separated by 40-100m of vegetated and/or broken marsh. To account for the spatial heterogeneity, I collected multiple samples from each pond; 3 replicate measurements 1m inland from the pond-marsh interface and 3 reference measurements 10m into the marsh behind those. This resulted in a total of 36 (3 study areas * 2 pond types * 2 distances from pond edge * 3 replicate samples) measurements of each indicator.

2.7 Soil strength

We measured soil shear strength to infer the erodibility of marsh soils surrounding ponds, a property important in mechanical, or physical erosion. A Humboldt H-4227 Shear Vane was inserted at various depths and pivoted until the soil failed and the peak strength of the soil was recorded on the handle gauge (Figure 3). I took readings at 55cm, 35cm, 25cm, and 10cm below the marsh surface and recorded the values in a field book to later be scaled with the blade-size in use. I replicated this measurement twice in very close proximity to account for local heterogeneity. Values were used to create a soil strength profile and capture the strength of soil below and above the vegetation rooting stratum which rests around 30cm. The measurements provide finer depth resolution than those measured by Schepers for his Blackwater NWR soil strength study (Schepers, 2017b).



Figure 3 – Humboldt Shear Vane with various measurement depths taped in red. Handle gauge to left of hand in photo.

2.8 Biomass

We measured plant height and above-ground biomass in 25cm by 25cm plots at each site to understand plant productivity and species compositions surrounding ponds, factors that can indicate marsh health and ability to compete with SLR. I chose representative plots due to the variation in species type within small areas of marsh. After I recorded the 5 tallest shoots in each plot, all standing biomass within the square plot was clipped at its base and stored in a bag on ice until lab processing occurred. In the lab, I sorted samples by living or dead fractions, and further divided the living biomass by species. *Distichilus spicata* and *Spartina patens* were not differentiated due to their similar morphological and productivity traits. Once sorted, biomass was dried at 70°C for 1 week and weighed to attain a dry mass. Species counts were used to calculate Simpson's Diversity Index, which incorporates the total count of species and the abundance of each to yield a value from 0 – 1, with 1 being most diverse.

$$D = 1 - \left(\frac{\sum n(n-1)}{N(N-1)} \right)$$

Simpson's Diversity Index – n = number of samples of a certain species. N = total number of samples.

2.9 Porewater chemistry

To understand the potential biogeochemical drivers of pond stability, I collected and processed porewater from the marsh soil to measure Hydrogen sulfide (H_2S) and Ammonium (NH_4^+) concentrations. These compounds help determine water quality and decomposition conditions. Bacteria associated with the decay of organic matter reduce sulfate into hydrogen-sulfide (H_2S), thus the concentration of H_2S in the porewater can be used as a proxy for decomposition rates in soil. High decomposition rates at the edge of a pond may indicate weakened soils and may be early indicators of pond expansion. NH_4^+ is partially derived from Nitrogen mineralization and can be a useful indicator of organic versus inorganic Nitrogen availability. Higher concentrations of inorganic Nitrogen compounds like NH_4^+ or Nitrate (NO_3^-) indicate limited uptake by plants – a potential sign of stressed vegetation. To collect porewater, we inserted a hollow metal rod with one end sealed and slotted for 2cm to a depth of 15cm below the marsh surface. A syringe with a 3-way stopcock attached to the other end of the rod allowed us to extract the water from pores of soil beneath the marsh surface. Once in the syringe, water was filtered through a 45-micron filter to remove organic particulates and dispensed into a Zinc Acetate fixing agent for later laboratory analysis (Figure 4). In the lab I added an H_2S indicator to the solution and ran samples through a Spectrophotometer to determine concentrations of H_2S (Method adapted from Cline, 1969). I collected ammonia samples through the same device and from the same sample site. Instead of fixing the solution, ammonia samples were stored on ice in the field and remained frozen until analysis. Samples were spiked with sulfuric acid and sparged for 8 minutes to remove Hydrogen Sulfide gas, then analyzed for ammonia concentrations through the Lachat QuikChem FIA+ (Figure 4). Results were subsequently drift-corrected to account for instrumental noise.



Figure 4 – (Left) Extracted porewater filtering through 45-micron filter and stored in 50mL tube for later Ammonium testing. Porewater used for sulfide levels was stored in smaller prepared scintillation vials. (Right) Water samples being sent to Lachat analyzer post spiking and sparging.

Results

3.1.1 – Changes in Pond area

Total ponded area increased in each study area at each time step. Study Area 1 (SA1) exhibited the greatest change with a ponded area of 100,732 m² in 1938 quadrupling to 402,588 m² in 2010. Ponded area in Study Area's 2 and 3 grew from 133,709 m² to 354,430 m² and 254817 m² to 52837 m² respectively (Figure 5). Most ponds that existed in 1938 merged with surrounding ponds to form larger ponds, excluding the central pond in each study area (Figure 6).

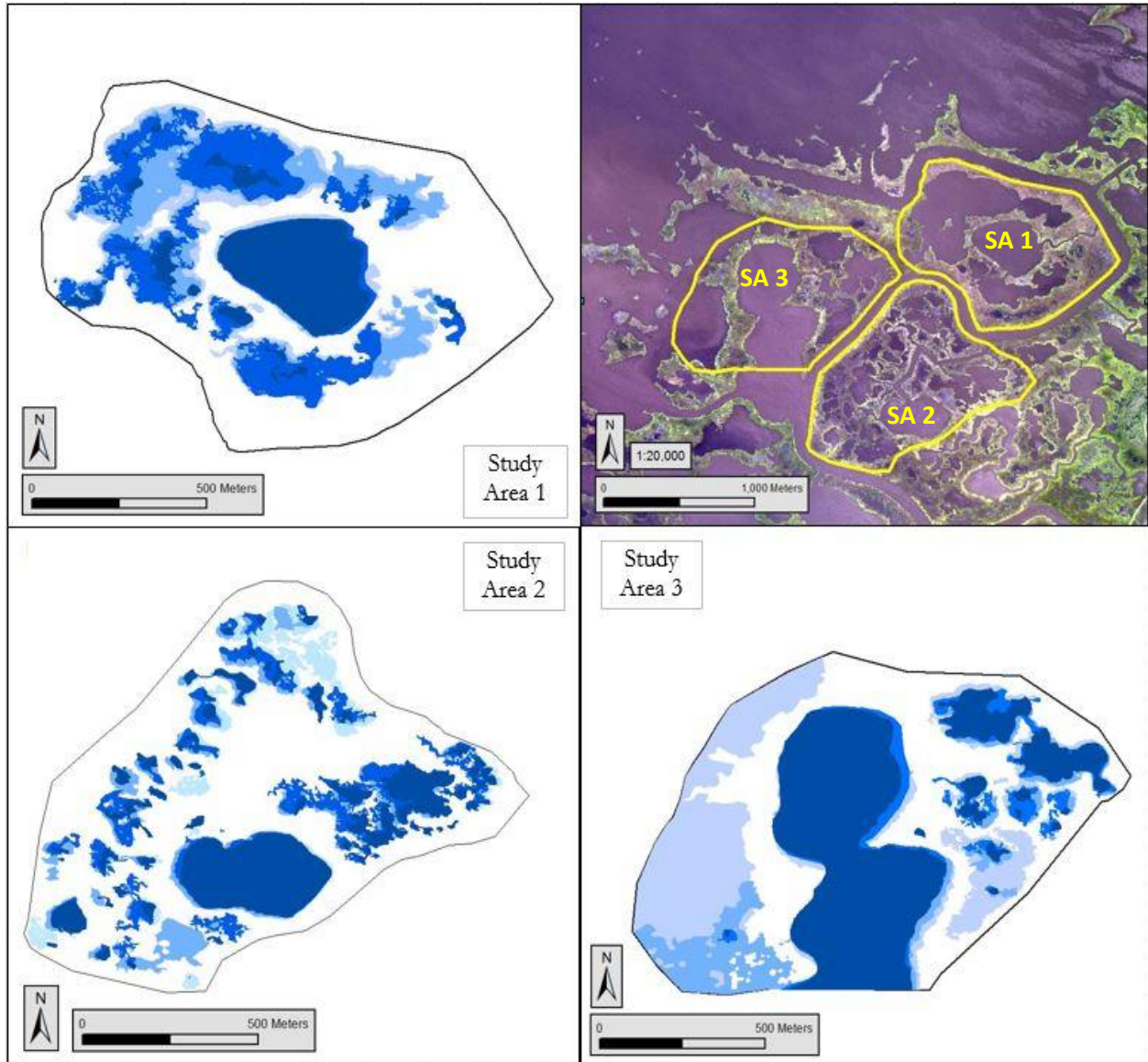


Figure 5 – Pond polygons through time at each study area. Darker shades of blue indicate older pond boundaries, delineated at four timesteps. (Top Right) - Overview map with false-color 2015 aerial imagery.

The total number of ponds remained relatively consistent in Study area's 1 and 3 after an initial doubling between 1938-1960. Study area 1 hovered around 35 ponds, while Study area 3 ultimately contained 42 ponds. Study area 2 held a consistent number of ponds up until the 1981-2010 timestep when the total number of ponds jumped from 36 to 124 (Figure 6).

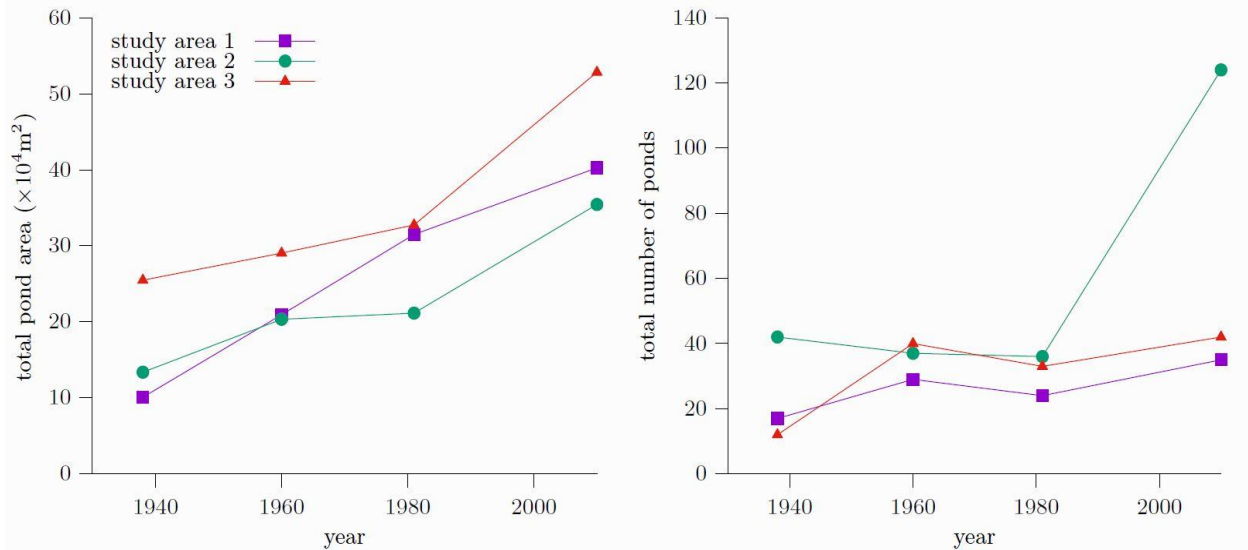


Figure 6 – total pond area and total number of ponds greater than 50m² at each timestep and for each study area. Poned area consistently increases, while total number of ponds generally remains

3.1.2 Pond size distributions

At each timestep and in each study area there is a greater number of small ponds (<1000m²) than large ponds (>1000m²). As time progresses, the number of small ponds decreases and the average pond size increases. In Study area 1, the 17 ponds with an average size of 5925m² that I recorded in 1938 merged with new ponds and each other to ultimately form 4 ponds with average size of 93824 m² in 2010. As time progresses, total ponded area increases as represented by the shaded areas below histograms (Figure 7).

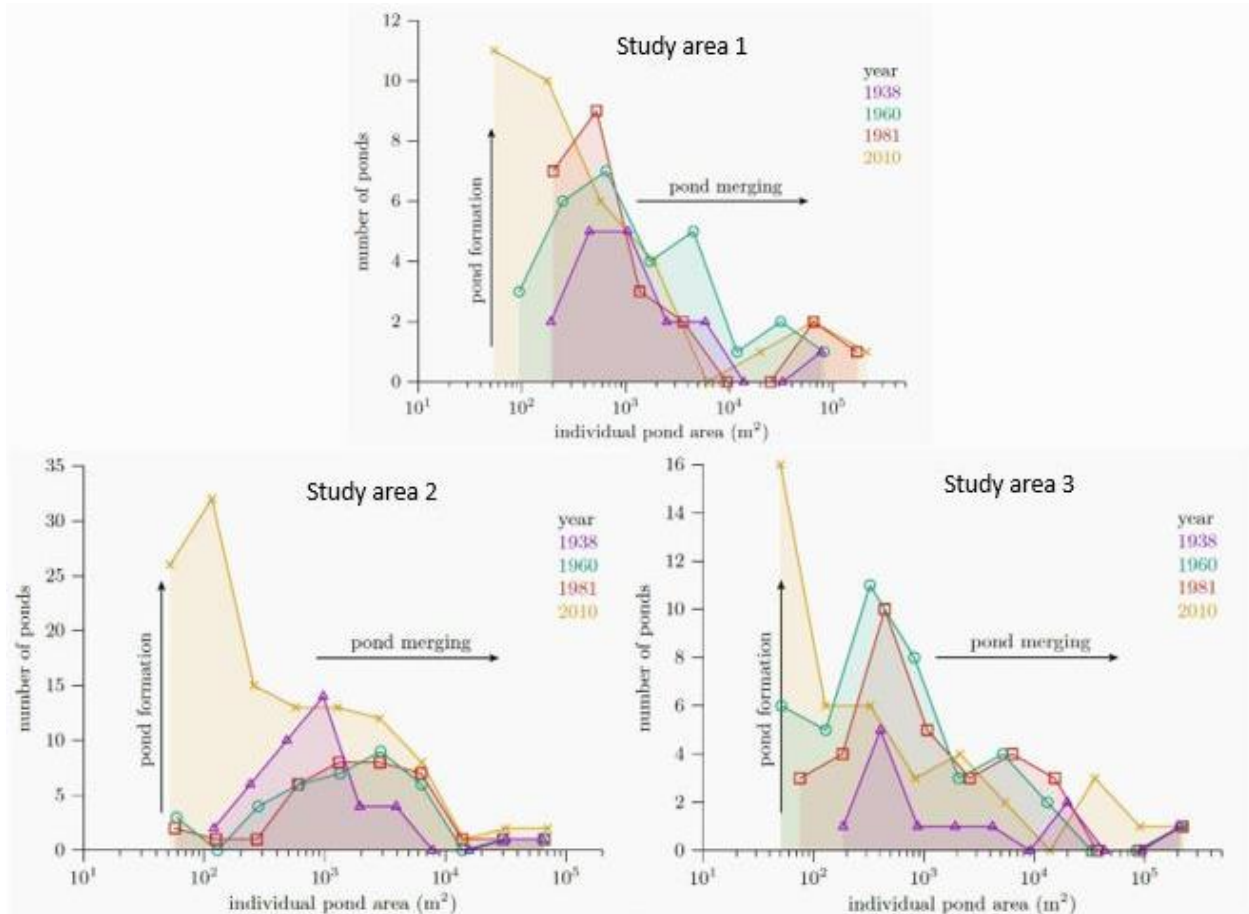


Figure 7 – Pond size distribution histograms. Every pond > 50m² within one of the three study areas is represented in this figure. Note that the vertical axis is scaled differently between study area based, and the horizontal axis is in logarithmic form. Shaded area below curves approximates total ponded area for a given time and study area. Colors represent year.

3.1.2 Expansion vs Merging Growth Rates

The growth of ponded area in SA1 and SA3 was dominated by merging mechanisms when total growth rates – the sum of expansion and merging growth rates – were high (>1000m² per pond per year). For example, in SA3 between 1981-2010, ponds grew an average of 1431m² each due to merging and only 264m² each by singular growth (Figure 8). In SA1 from 1960-1981, each pond grew an average of 1685m² due to merging mechanisms. For lower total growth rates, the distinction between expansion and merging mechanisms was less pronounced.

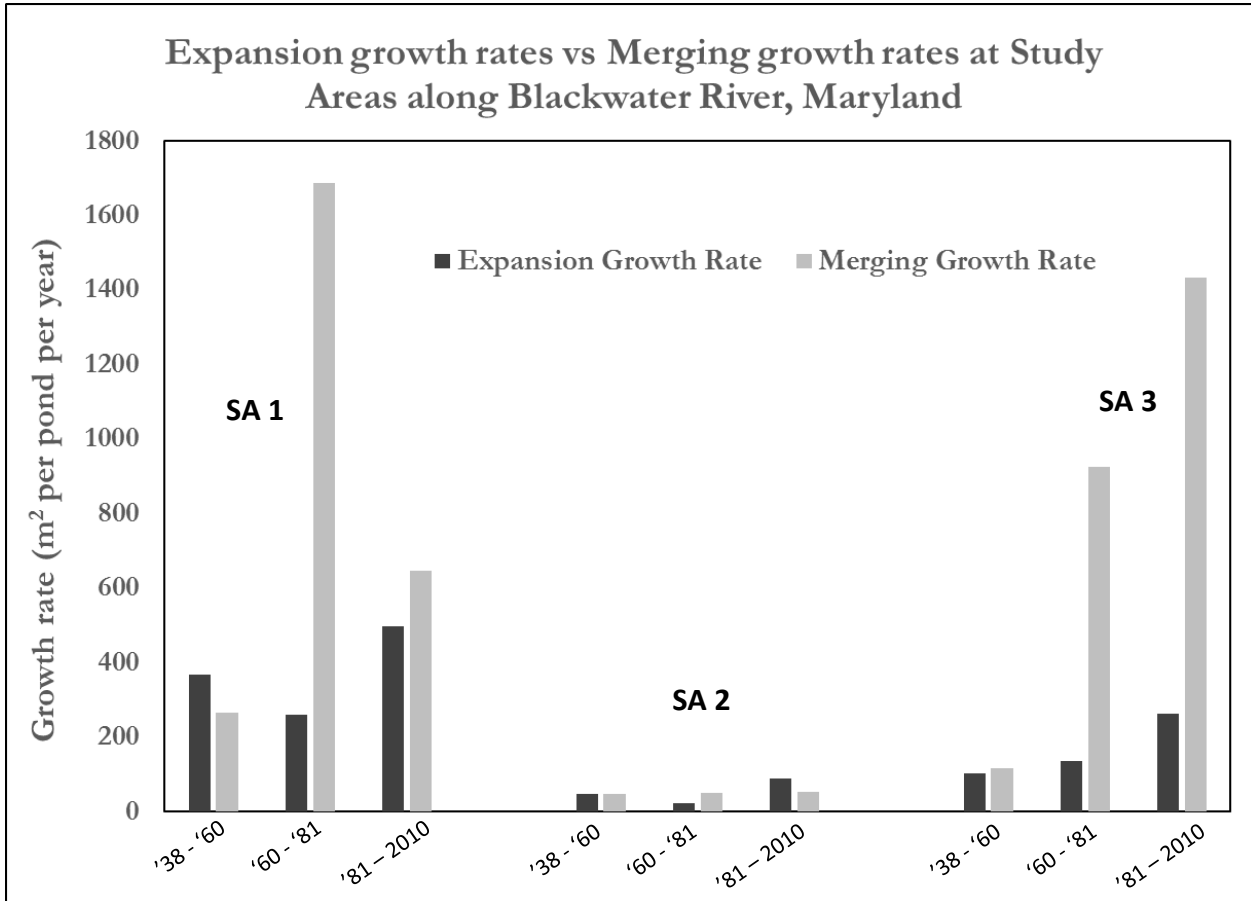


Figure 8 – Growth rate averaged per identified pond in each study area. In cases of rapid marsh loss, pond growth due to merging is the dominant mechanism.

3.1.3 – Non-merging ponds growth rates

Ponds that did not merge with others between a timestep exhibited a decreasing linear growth rate with size. The linear growth rate represents the average rate at which a pond edge replaces the adjacent marsh and is calculated by finding the difference in the square root of the final pond size and square root of the initial pond size over a given timestep. Edges of small (<5,000 m²), often young ponds expanded up to 1.56 m/yr while larger ponds (>10,000 m²) grew slower with a maximum rate of .43 m/yr. At the margin of the expansive (~18,000,000 m²) Lake Blackwater, edge growth rate increases to an average rate of 0.88 m/yr (Figure 9).

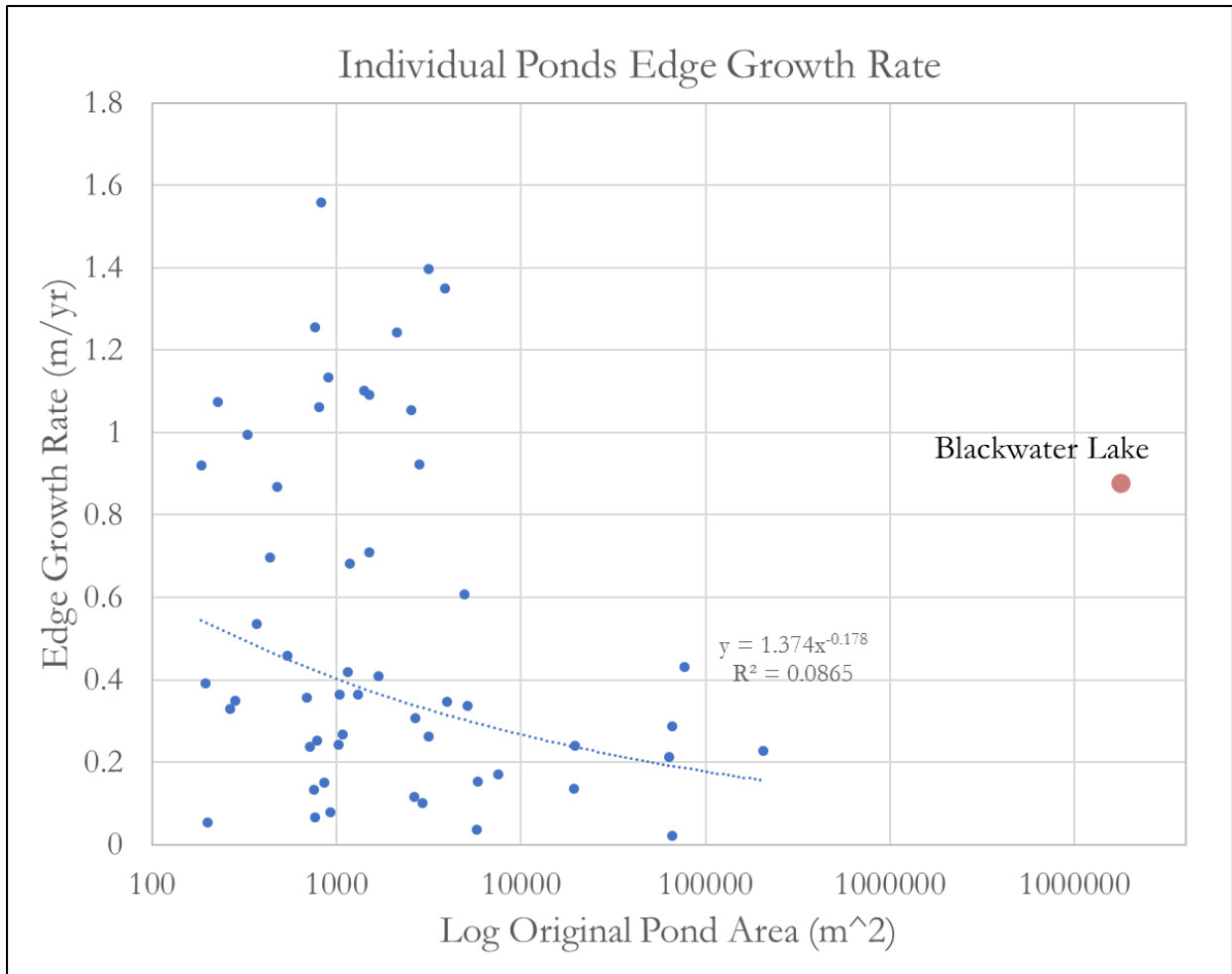


Figure 9 – Linear edge growth rates (m/yr) vary by an order of magnitude and tend to be more rapid in smaller ponds. Each dot represents the average edge growth of an individually tracked pond during an observed timestep. Orange dot represents linear edge retreat rate at the southeast margins of Lake Blackwater.

3.2 Characteristics of stable and unstable ponds

Total live aboveground biomass adjacent to stable and unstable ponds averaged $841 \pm 98 \text{ g/m}^2$ and $607 \pm 110 \text{ g/m}^2$ respectively. Biomass collected 10m into the marsh away from a pond's edge exhibited similar trends, with an average of $\sim 400 \text{ g/m}^2$ more living biomass near stable ponds than unstable ponds. Simpson's Diversity Index resulted in a value of .73 and .82 for all living aboveground vegetation collected at the edge of stable and unstable ponds respectively, signifying higher diversity around unstable ponds. Samples were collected in mid-august 2017 and capture annually high biomass values.

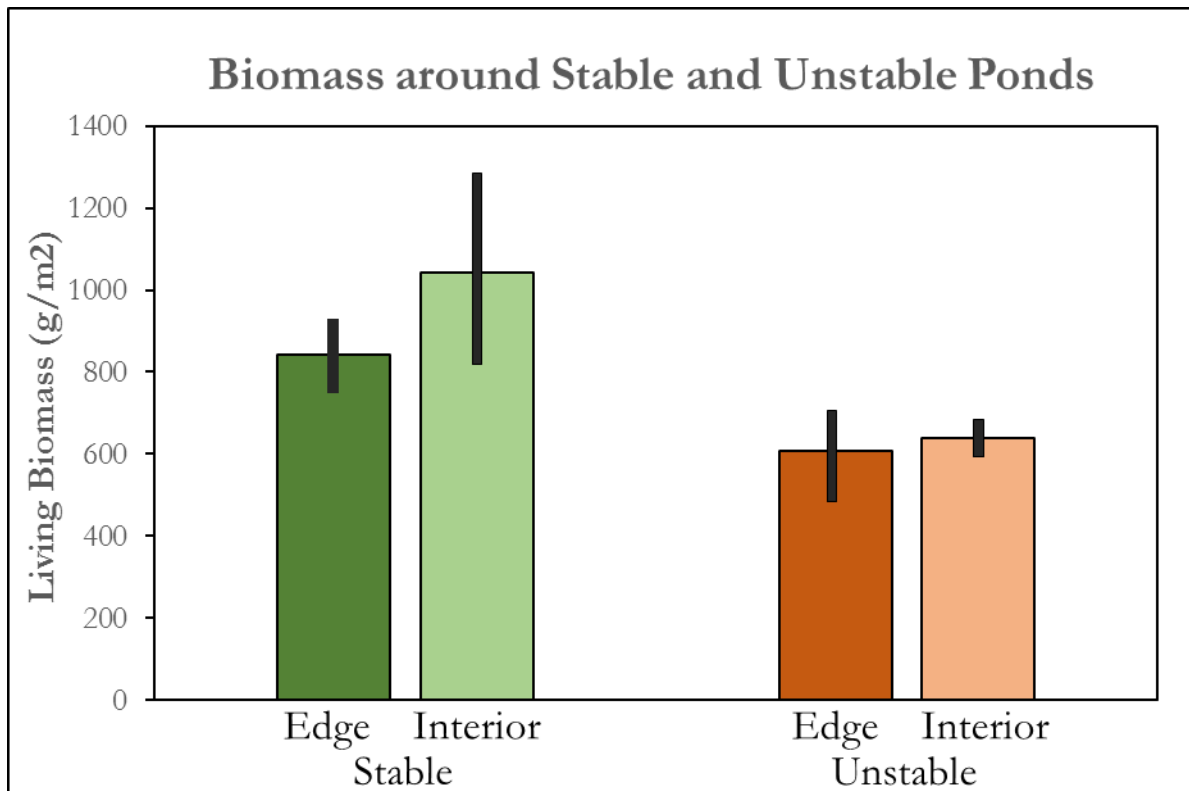


Figure 10 - Each bar represents the average of all measurements ($n=9$) collected at a certain pond type and location. Error bars represent 2σ .

Sulfide levels in porewater extracted from 15cm beneath the marsh surface were twice as concentrated around unstable ponds as levels around stable ponds ($\mu_{\text{unstable}} = 6.4 \pm 0.8 \text{ mM}$, $\mu_{\text{stable}} = 3.2 \pm 0.5 \text{ mM}$). Porewater ammonia – the product of the mineralization or ammonification of organic nitrogen – exhibited a similar concentration trend, with higher values around unstable ponds than stable ponds ($\mu_{\text{unstable}} = 161 \pm 29 \text{ }\mu\text{M}$, $\mu_{\text{stable}} = 97 \pm 38 \text{ }\mu\text{M}$). (Figure 11). I noted no trends between pond sampling locations (edge versus interior).

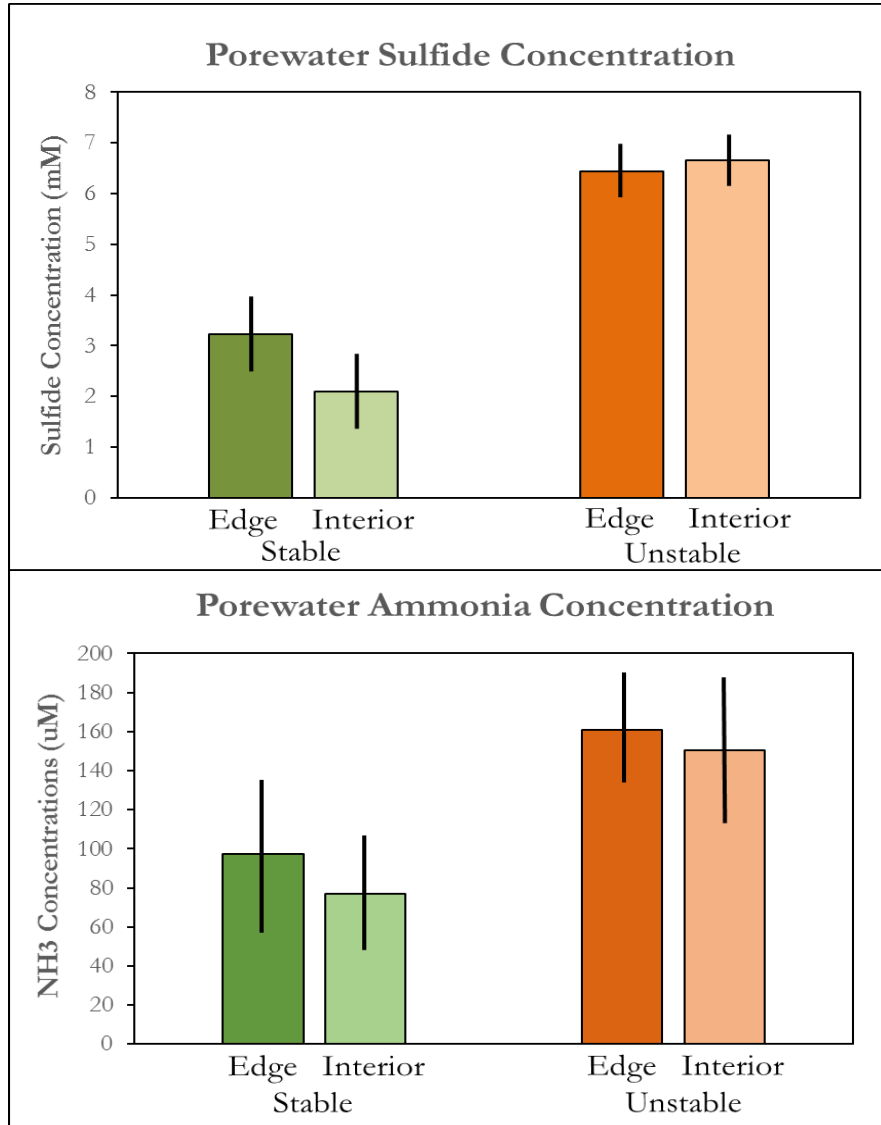


Figure 11 - Data bars represent average (n=9) values, error bars show +/- one standard error. Concentrations for sulfide in milliMolar, while concentrations for ammonia/ammonium are in micromolar. Green represents stable ponds and orange represents unstable ponds, with darker shades representing conditions at the edge of ponds.

Soil strength values decreased dramatically between the measurement depths of 10cm and 25cm. Values remain steady from 25cm to 35cm, but all slightly increase at the deepest measurement depth of 55cm (Figure 12). Average soil strength at a depth of 10cm was higher around each stable pond than around the nearby unstable pond despite similar trends in their vertical profiles and similar shear strengths below the rooting zone. Rooting depth is illustrated at a maximum 30cm as suggested by previous research in the Blackwater NWR (Scheppers, 2017b).

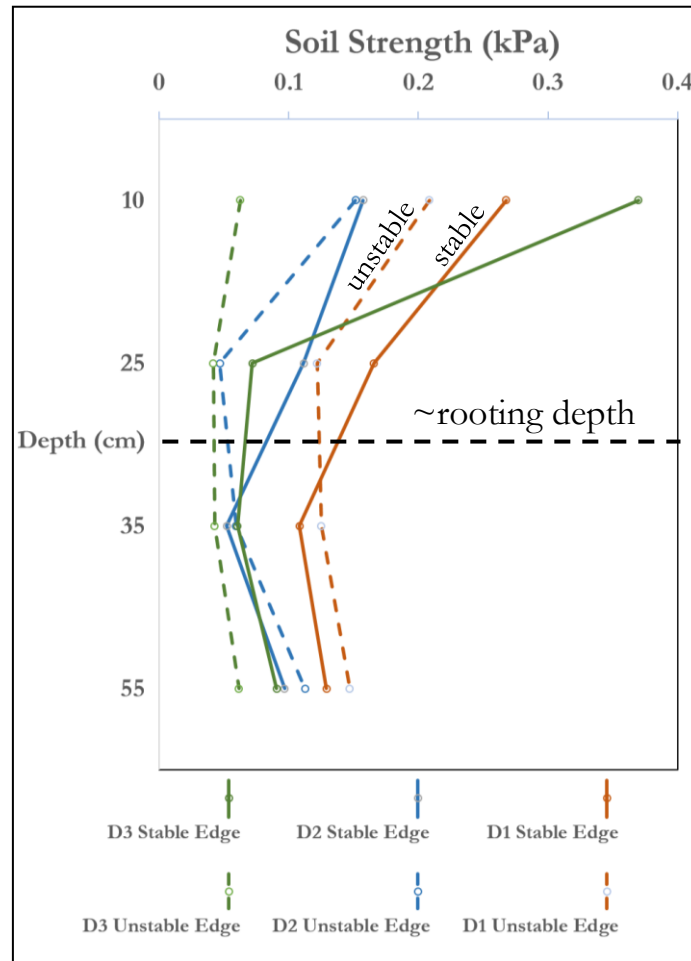


Figure 12 - Each node on a strength profile represents the average of replicate samples (n=3). Solid lines represent stable pond soils while dashed lines represent unstable pond soils. Matching colors indicate ponds within a study area.

Discussion

The Blackwater NWR continues to experience an expansive conversion of vegetated marsh into unvegetated ponds. The interaction of biogeochemical and physical factors is important in determining the future of the wetland and the rate of change therein. Previous studies suggest a bleak future for the refuge; low tidal range and inorganic suspended sediment concentrations make them vulnerable to accelerating SLR (Kirwan and Guntenspergen, 2010; Mariotti, 2016; Kearney and Turner, 2016). While I observe the greatest amount of vegetation die-off at the northwest reaches of the Blackwater River, some reaches of marsh around stable ponds remain relatively intact (Schepers, 2017). To assess why some of these ponds remain stable while others grow rapidly, I holistically combined remote sensing analyses with field measurements. This study marks the first investigation of the behavior of individual ponds within the Blackwater NWR, and the most comprehensive analysis of individual pond growth anywhere.

Once formed, a pond may expand or recover depending on various factors such as water nutrient and sediment concentrations and surrounding vegetation health. In Blackwater, the most visually apparent pattern is pond formation followed by expansion and ultimately merging. In Blackwater, almost all ponds expand and lead to permanent marsh loss (Stevenson et al., 1985). In contrast, ponds in the saltmarshes of coastal Massachusetts underwent contraction and expansion at nearly equal rates with ponds dynamically merging and splitting (Wilson et al., 2009). Marshes there receive higher minerogenic sediment input, experience greater tidal fluctuations, and exhibit more resilience to SLR over the past century.

We propose that ponds in the Blackwater NWR nucleate as small depressions in the inner marsh platform, far from hydrological connections, and propagate outward through time (Schepers, 2017). Ponds are often underlain by marsh peat, implying their secondary nature in an otherwise vegetated marsh system (Wilson et al., 2009). Waterlogging stress rapidly degrades soils and plants surrounding the depression and eventually decomposes the underlying root mat (Redfield, 1972). As the root network decays, sediment is open to export during tidal-flushing events. More roots become exposed to the stagnant and often toxic pond waters, widening the region of die-off. The process may continue until a connection, whether manifested as sub-surface or aerially exposed tidal channels, acts to refresh the stagnant pooled water. In Blackwater most ponds enlarge and within several decades intersect tidal channels or merge with other connected pools. This connected stage enables fresher waters, the flushing of phytotoxins, and higher suspended sediment concentrations in medium sized ponds, a potential cause of their lessening expansion rates with increasing ponds size (Figure 9).

Often pond growth results in the merging of ponds which I note here as a primary contributor to marsh loss. The distribution of ponds through time and space reiterates this pattern as I see a high number of small water bodies surrounding several large water bodies. Ponds are constantly forming, growing, and merging with adjacent ponds to ultimately result in the few large water bodies currently present in Blackwater (Figure 5). The data also reveals a pattern of more small ponds emerging nearer to present time, as various stresses including SLR promote pond nucleation in hydrologically isolated reaches of the marsh platform (Figure 7). Study area 2 experienced a proliferation of small ponds between 1981 and 2010. The die-off gradient explained by Schepers et al. (2016) suggests that Study area 2 would be the last of the

three to experience the shift to highly ponded marsh, a potential explanation for its recent pond formation rates.

Merging, the visual and hydrologic conjoining of two or more ponds, is the primary contributor to marsh loss especially when loss is large. In Study Area 1 (SA1), where the average pond grew $\sim 2000 \text{ m}^2/\text{year}$ from 1960-1981, $1700 \text{ m}^2/\text{year}$ is attributable to merging (Figure 8). The overall increase in pond area in the refuge concurs with findings from studies on other salt marshes, however the pace of change in Blackwater is more rapid than is observed on other saltmarshes (Kearney et al., 1988; Wilson et al., 2009). The increase in merging growth rates in the latter two timesteps (Figure 6) agrees with a study of the coastal Massachusetts saltmarshes, which also showed an increase in merging events since 1977 (Wilson et al., 2009). The high marsh die-off rates observed in the refuge are enabled by a continuous pattern of pond formation, expansion, and merging. This sequence presents itself on the marsh surface as irregularly shaped ponds, the products of merging, adjacent to smaller recently formed pools. Merging is recorded when surficial connections are apparent, but previous studies have recognized its initiation from subsurface connections – meaning my merging rates may underestimate hydrologic connectivity in Blackwater NWR (van Huissteden and van de Plassche, 1998).

Poorer growing conditions – as suggested by porewater chemistry and biomass – for plants surrounding unstable ponds suggests that biochemical mechanisms are drivers of marsh loss (Nyman et al., 1994). Most ponds in the Refuge expand consistently through times, and worse biogeochemical conditions lead to a less stable marsh. My study focused on the growth of individual ponds at various sizes and ages, and the few ponds that grow slowly through time are large and have existed since at least 1938. Pond size partially determines the physical mechanisms which may act ponds, with bodies exceeding a critical width in the dominant wind direction experiencing wind-driven wave impacts at their margins (Mariotti and Fagherazzi, 2013; Ortiz et al., 2017). In Blackwater few ponds appear to reach this critical width and most grow through biogeochemical die-off at their margins. I document small, early-life ponds as less stable and quicker growing than larger, previously developed ponds; I recorded faster edge growth rates in ponds $100 - 10,000 \text{ m}^2$ than in ponds $10,000 - 100,000 \text{ m}^2$ (Figure 9). Lake Blackwater was the only water body that appeared to exceed the critical-fetch width in the dominant wind direction as it was the only large water body to show an increase in edge growth rate (Figure 9) (Mariotti and Fagherazzi, 2013; Ortiz et al., 2017; Schepers, 2017b). In other marshes, wind-driven wave erosion is likely dominant in water bodies smaller than Lake Blackwater as the widths for the onset of runaway erosion is 200-1000 m in US Atlantic marshes (Mariotti and Fagherazzi, 2013) – but few ponds of this size and exist in Blackwater. Another factor limiting the impact of wave erosion in the Refuge is the shallow depth of the bodies, as wave action increases with water depth (Temmerman et al., 2005).

Vegetation interacts dynamically with physical mechanisms to stabilize saltmarshes. Abundant vegetation creates an expansive, erosion-resistant root network belowground and slows water-movement aboveground, promoting sedimentation and vertical upkeep of the marsh platform. The stability of studied ponds in Blackwater is reflected in their relative abundance of biomass, where stable marshes had higher biomass than unstable marshes. Blackwater marshes are colonized by the low-marsh species *S. americanus* and *S. alterniflora*

and the high-marsh *S. patens* and *D. spicata*. Though no one species was dominant around stable or unstable ponds, species composition did vary slightly. The higher Simpson's Diversity Index for vegetation at the margins of unstable versus stable ponds (.82 versus .73) indicates more plant diversity around unstable ponds. A more homogenous plant community implies that more consistent growing conditions allow similar plants to thrive and outcompete less fit species. Even with the slight difference in diversity indices, all sampling sites exhibited poor growing conditions; the marsh in Blackwater is heterogenous and fragmented. Previous plant biodiversity studies in Blackwater found no clear species abundance shift with die-off proportions but did suggest that species mixing was correlated with increasing marsh loss (Scheppers, 2017b). For the regions of the Refuge experiencing the greatest die-off, vegetation abundance and diversity are valuable indices to monitor when predicting future biogeomorphic changes.

Porewater sulfide and ammonia levels act as useful tools for understanding variation in species composition and plant productivity and are influenced by both local hydrology and drainage frequency as well as in-situ biogeochemical processes. They reflect soil conditions such as decomposition rates and nutrient abundances. Both sulfide and ammonia levels were twice as concentrated in soils adjacent to unstable ponds than in those around stable ponds (Figure 11). Sulfate reduction in anaerobic soils, like those that surround the persistently water-filled pond basins, yields sulfide. Accumulation of sulfide in porewater – especially at depths coinciding with the mesohaline vegetation's rooting zone – is known to affect plant fitness and brackish ecosystem functions (Lamers et al., 2013). Sulfide is shown through field and laboratory studies to be toxic above levels of 1-3 mMolar for the saltmarsh plant *Spartina alterniflora*, a concentration far exceeded in soils around unstable ponds and even those around many stable ponds in Blackwater (Lamers et al., 2013). A study by Van Huissteden et al. (1998) on the Great Marshes of Cape Cod, USA, hypothesized that degradation of organic matter by sulfate reducing bacteria is a primary cause of pond growth. The negative impacts of sulfide, sometimes referred to as a phytotoxin, include its prevention of root uptake of inorganic nutrients such as Nitrogen (Swarzenski et al., 2008). This effect may partially explain the increased Ammonium (NH_4^+) in soils with high sulfide levels. Ammonium is also sourced from respiration by anaerobic bacteria involved in processes like Nitrogen mineralization and can be removed from soils by plant uptake of Nitrogen and nitrification-denitrification. Due to poor water drainage, hypoxic soils, and high sulfide levels, ammonia (NH_3) levels remain high around unstable ponds. Though no specific water flux measurements were recorded during my field campaign, the unstable ponds sampled often lacked surficial connection to a tidal channel and thus their surrounding pond water likely has a higher residence time enabling sulfide and ammonium accumulation.

Soil strength measurements suggested more erodible soils around unstable ponds and at depths near or below the active rooting zone. Scheppers et al. (2017b) showed that, despite weak near-surface soils in the Blackwater marshes relative to more peat-dense saltmarshes, their strength in the rooting zone is still far higher than the critical shear stress inflicted by typical currents and waves. Beneath this cohesive surface layer rests weaker, unbound sediments prone to export due to water currents or wave-action. This is expressed in the low shear strength values of $\sim 0.1\text{kPa}$ lower in the strength profiles. The low critical shear stress

needed to suspend and remove these weak soils likely mirrors conditions at the bottom of ponds, which often exhibit a loose “ooze” layer to be exported when a pond gains tidal connection (Ganju et al. 2013, 2017). While wind-driven lateral erosion does not seem to be a critical pond growth mechanism in the Refuge except in Lake Blackwater, the potential for high-wave power is greater in larger ponds. During storm events, surge waves could erode bare patches or export sediment from below the rooting zone (Schepers, 2017b). Perhaps an equally important impact of the strength differential above and below the rooting zone is cantilever processes. The erodibility gradient enables failure of the cohesive sediments surface soils when their underlying material is removed, hastening lateral erosion (Bendoni et al., 2016). Scarps and failure blocks are not as prominent in Blackwater as in other Atlantic marshes with larger tidal ranges, but I did record overhangs at the banks of most tidally connected ponds. Despite potential for physical mechanisms to expand ponds large ponds, the consistent growth of total ponded area and unhealthy growing conditions at each Blackwater study area over the past 80 years suggests biogeochemical processes play a more significant role in marsh die-off and pond expansion here than do physical ones.

Conclusions

My findings demonstrate that the vulnerable wetlands of the Blackwater National Wildlife Refuge in Maryland, USA, are threatened by vegetation die-off, pond formation, and pond expansion. By combining remote sensing analyses of historic imagery with contemporary field studies I attempt to explain the pattern and processes of marsh loss associated with ponding. During periods of drastic pond expansion, most growth was attributed to pond merging patterns, a process dependent on the formation and subsequent coalescing of small to medium sized ponds. These lesser sized ponds tend to be less stable due to their hydrologic isolation and stagnant water conditions deteriorating surrounding vegetation and root mats. Considering the inferior biochemical conditions around unstable ponds and the lack of wind-driven erosion in almost all Blackwater ponds, biogeochemical processes appear responsible for the majority of pond expansion and marsh loss along in the Blackwater NWR.

Acknowledgements

I would like to thank all of the mentors, colleagues, and friends that have helped me over the past several years; Matt Kirwan for advising me and at every turn and encouraging concise and communicable science, Ellen Herbert and Orencio Vinent Duran for consistently taking time to direct my methodology and clarify my goals, Lennert Schepers for his previous studies and materials on ponding in the Blackwater NWR and willingness to collaborate, David Walters for his essential role in field sampling, and the rest of the Kirwan Lab for their comradery and support. I would also like to extend my gratitude to Greg Hancock for his mentorship throughout my undergraduate years along with the rest of the Geology faculty who encourage and inspire their students all while having more fun than any other department on campus. Finally, this research would not be possible without funding from the NSF and USGS who enable scientific progress even in rough waters.

References Cited

- Adamowicz, S.C., and Roman, C.T., 2005, New England salt marsh pools; a quantitative analysis of geomorphic and geographic features: *Wetlands* (Wilmington, NC), v. 25, p. 279-288.
- Bendoni, M., R. Mel, L. Solari, S. Lanzoni, S. Francalanci, and H. Oumeraci. 2016. Insights into lateral marsh retreat mechanism through localized field measurements. *Water Resour. Res.* **52**: 1446–1464. doi:10.1002/2015WR017966
- Cline, J. 1969, Spectrophotometric determination of hydrogen sulfide in natural waters. *Limnology Oceanography*. 14: 454-456.
- Costanza, R., Pérez-Maqueo, O., Martinez, M.L., Sutton, P., Anderson, S.J., and Mulder, K., 2008, The value of coastal wetlands for hurricane protection: *AMBIO: A Journal of the Human Environment*, v. 37, p. 241-248.
- Day, J. W., G. P. Kemp, D. J. Reed, D. R. Cahoon, R. M. Boumans, J. M. Suhayda, and R. Gambrell. 2011. Vegetation death and rapid loss of surface elevation in two contrasting Mississippi delta salt marshes: The role of sedimentation, autocompaction and sea-level rise. *Ecol. Eng.* 37: 229–240. doi:10.1016/j.ecoleng.2010.11.021
- Ganju, N. K., Z. Defne, M. L. Kirwan, S. Fagherazzi, A. D’Alpaos, and L. Carniello. 2017. Spatially integrative metrics reveal hidden vulnerability of microtidal salt marshes. *Nat. Commun.* **8**: 14156. doi:10.1038/ncomms14156
- Ganju, N. K., N. J. Nidzieko, and M. L. Kirwan. 2013. Inferring tidal wetland stability from channel sediment fluxes: Observations and a conceptual model. *J. Geophys. Res. Earth Surf.* **118**: 2045–2058. doi:10.1002/jgrf.20143
- Hartig, E.K., V. Gornitz, A. Kolker, F. Mushacke, and D. Fallon. 2002. Anthropogenic and climate change impacts on salt marshes of Jamaica Bay, New York City. *Wetlands* 22: 71–89.
- Kirwan, M.L., Walters, D.C., Reay, W.G., and Carr, J.A., 2016, Sea level driven marsh expansion in a coupled model of marsh erosion and migration: *Geophysical Research Letters*, v. 43, p. 4366-4373, doi: 10.1002/2016GL068507.
- Lamers, L. P. M., Govers, L. L., Janssen, I. C. J. M., Geurts, J. J. M., Van der Welle, M. E. W., Van Katwijk, M. M., ... Smolders, A. J. P. (2013). Sulfide as a soil phytotoxin—a review. *Frontiers in Plant Science*, 4, 268. <http://doi.org/10.3389/fpls.2013.00268>
- Leonardi, N., Defne, Z., Ganju, N.K., and Fagherazzi, S., 2016, Salt marsh erosion rates and boundary features in a shallow Bay: *Journal of Geophysical Research: Earth Surface*, v. 121, p. 1861-1875.

- Leonardi, N., and Fagherazzi, S., 2014, How waves shape salt marshes: *Geology*, v. 42, p. 887-890.
- Mariotti, G., and Fagherazzi, S., 2013, A two-point dynamic model for the coupled evolution of channels and tidal flats: *Journal of Geophysical Research: Earth Surface*, v. 118, p. 1387-1399, doi: 10.1002/jgrf.20070.
- Mariotti, G., and Fagherazzi, S., 2013. Critical width of tidal flats triggers marsh collapse in the absence of sea-level rise. *Proceedings National Academy of Science U. S. A.* **110**: 5353–6. doi:10.1073/pnas.1219600110
- Mariotti, G., 2016, Revisiting salt marsh resilience to sea level rise: Are ponds responsible for permanent land loss? *Journal of Geophysical Research: Earth Surface*, v. 121, p. 1391-1407, doi: 10.1002/2016JF003900.
- National Ocean Service, 2015, Sea Level Trends:
(https://tidesandcurrents.noaa.gov/sltrends/sltrends_station.shtml?stnid=863762412/42016).
- National Ocean Service, 2013, National Coastal Population Report: NOAA, Report March 2013, 1-20 p.
- Nyman, J.A., Carlross, M., DeLaune, R., and Patrick Jr, W., 1994, Erosion rather than plant dieback as the mechanism of marsh loss in an estuarine marsh: *Earth Surface Processes and Landforms*, v. 19, p. 69-84.
- Pethick, J., 1992, Saltmarsh geomorphology: *Saltmarshes: Morphodynamics, Conservation and Engineering Significance*, p. 41-62.
- Pethick, J.S., 1974, The Distribution of Salt Pans on Tidal Salt Marshes: *Journal of Biogeography*, v. 1, p. 57-62, doi: 10.2307/3038068.
- Ramsey, E.W., and Laine, S.C., 1997, Comparison of Landsat Thematic Mapper and High Resolution Photography to Identify Change in Complex Coastal Wetlands: *Journal of Coastal Research*, v. 13, p. 281-292.
- Rocchio, L., 2017, Blackwater National Wildlife Refuge:
(<https://landsat.visibleearth.nasa.gov/view.php?id=7928704/20172017>).
- Schepers, L., Kirwan, M., Guntenspergen, G., and Temmerman, S., 2017, Spatio-temporal development of vegetation die-off in a submerging coastal marsh: *Limnology and Oceanography*, v. 62, p. 137-150.

- Schepers, L., 2017b, Spatial patterns and bio-geomorphological effects of vegetation loss in a submerging coastal marsh [Ph.D. thesis]: Antwerp, Belgium, University of Antwerpen.
- Weier, J., and Herring, D., 2000, Measuring Vegetation (NDVI & EVI): (<http://earthobservatory.nasa.gov/Features/MeasuringVegetation/>Feb 5 2017).
- Wilson, C.A., Wilson, C.A., and Hughes, 2014, Saltmarsh pool and tidal creek morphodynamics: Dynamic equilibrium of northern latitude saltmarshes? *Geomorphology* (Amsterdam, Netherlands), v. 213, p. 99; 99-115; 115.
- Wilson, C.A., FitzGerald, D., and Hughes, Z., 2009, Microchannel and creek development in a New England saltmarsh, Rowley, Massachusetts: Abstracts with Programs - Geological Society of America, v. 41, p. 18.
- van Huissteden, J. and O. van de Plassche. 1998. Sulphate reduction as a geomorphological agent in tidal marshes ("Great Marshes" at Barnstable, Cape Cod, USA). *Earth Surface Processes and Landforms* 23: 223–236.